

Received: 2019.06.28
Accepted: 2019.09.17
Published: 2019.12.17

Computer-Based 3D Simulations to Formulate Preoperative Planning of Bridge Crane Technique for Thoracic Ossification of the Ligamentum Flavum

Authors' Contribution:
Study Design A
Data Collection B
Statistical Analysis C
Data Interpretation D
Manuscript Preparation E
Literature Search F
Funds Collection G

AC 1,2 **Chen Yan***
DE 1,2 **Huai-Cheng Jia***
DF 1,2 **Jia-Xi Xu***
B 3 **Tao Xu**
B 4 **Kun Chen**
A 1 **Jing-Chuan Sun**
AG 1 **Jian-Gang Shi**

1 Second Department of Spine Surgery, Changzheng Hospital, Navy Medical University, Shanghai, P.R. China
2 Undergraduate Incubation Center, Navy Medical University, Shanghai, P.R. China
3 Department of Orthopedic Surgery, No. 906 Hospital of the People's Liberation Army (PLA), Ningbo, Zhejiang, P.R. China
4 Department of Orthopedics, Guangzhou General Hospital of Guangzhou Military Command, Guangzhou, Guangdong, P.R. China

Corresponding Author:
Source of support:

* Chen Yan, Huai-Cheng Jia, and Jia-Xi Xu contributed equally to this study and should be considered as the co-first authors
Jing-Chuan Sun, Jian-Gang Shi, e-mail: changzhengspine@smmu.edu.cn

The study was supported by the Undergraduate Innovation Fund of Navy Military Medical University (Spine Surgery Department), National Natural Science Foundation of China (NO.81802218) and Shanghai Science and Technology Commission Technology support project (No.18441905800).

Background: The bridge crane technique is a novel surgical technique for the treatment of thoracic ossification of the ligamentum flavum (TOLF), but its preoperative planning has not been studied well, which limits the safety and efficacy of surgery to some extent. The purpose of this study was to investigate the method of application and effect of computer-aided preoperative planning (CAPP) on the bridge crane technique for TOLF.


Material/Methods: This retrospective multi-center included 40 patients with TOLF who underwent the bridge crane technique from 2016 to 2018. According to the utilization of CAPP, patients were divided into Group A (with CAPP, n=21) and Group B (without CAPP, n=19). Comparisons of clinical and radiological outcomes were carried out between the 2 groups.

Results: The patients in Group A had higher post-mJOA scores and IR of neurological function than those in Group B ($p<0.05$). Group A had shorter surgery time, fewer fluoroscopic images, and lower incidence of complications than Group B. In Group A, there was a high consistency of all the anatomical parameters between preoperative simulation and postoperative CT ($p>0.05$). In Group B, there were significant differences in 3 anatomical parameters between postoperative simulation and postoperative CT ($p<0.05$). In Group B, the patients with no complications had higher post-SVOR and lower SVRR and height of posterior suspension of LOC in postoperative CT than those in postoperative simulation ($p<0.05$).

Conclusions: CAPP can enable surgeons to control the decompression effect accurately and reduce the risk of related complications, which improves the safety and efficacy of surgery.

MeSH Keywords: **Computer-Aided Design • Neurosurgery • Spine • Spondylosis**

Full-text PDF: <https://www.medscimonit.com/abstract/index/idArt/918387>

 4192

 6

 5

 52



Background

Thoracic ossification of the ligamentum flavum (TOLF) is commonly considered as a primary contributor to thoracic myelopathy in East Asia [1–3]. Due to its progressive feature and poor efficacy for conservative therapy, surgical treatment is usually a preferred choice [4,5]. However, the clinical outcomes of surgical intervention are often unsatisfactory and its risk is also high, which is accompanied by various complications such as cerebrospinal fluid leakage and neurological deficit [6–9].

A novel surgical method named the bridge crane technique was proposed recently to reduce the incidence of complications and improve the efficacy of treatment of severe TOLF [10]. Its core concept lies in the isolation and suspension of the laminae-OLF complex (LOC) for direct decompression of the thoracic spinal cord without resection of the TOLF. Although the idea of the bridge crane technique might seem simple, there are still several unresolved problems in clinical practice. Firstly, the border of the ossified mass is irregular and it cannot be observed directly during the operation. If the range of isolation of LOC is insufficient, the residual ossified lesions can increase the risk of neurologic deterioration and recurrence [11–13]. Conversely, if the range of isolation of LOC is excessive, resection of the facet joints can cause kyphosis [14,15]. It is necessary to position the ossified mass precisely and determine the range of isolation before surgery. Secondly, the decompression effect mainly depends on the posterior shifting of the LOC. The distance of posterior shifting of the LOC is determined by the length of pedicle screws outside the bone, the amount of excision of the spinal processes, and the curvature and position of the transverse connectors. Insufficient length, amount of excision, or curvature can cause incomplete decompression. Conversely, if they are excessive, they can increase the risks of screw loosening and spinal instability [16]. Furthermore, excessive posterior shifting also might led to dural tears and cerebrospinal fluid (CSF) leakage [17]. Thirdly, the curvature of the longitudinal rods is closely related to the length of pedicle screws outside the bone at each level and the physiological curvature of thoracic spine. However, the curvature is not usually predictable and the surgeon has to bend the rods repeatedly for adaption to the screw grooves, which can increase the risk of rod breakage [18,19]. In clinical practice, it is difficult for surgeons to control so many parameters within appropriate ranges at the same time due to the lack of a quantitative analysis technique. More importantly, surgeons usually lack an effective method to measure the distance of posterior shifting of the LOC and to evaluate the decompression effect accurately during the operation, so the key to a successful operation is good preoperative planning.

Currently, computer-aided design (CAD) technology is applied in the preoperative planning of various surgeries due to its

low cost, individuation, accuracy, and repeatability [20–23]. Computer-aided preoperative planning (CAPP), which is based on three-dimensional (3D) anatomical reconstructions and quantitative data analysis, is gradually replacing the traditional approach based on 2D images and surgeon expertise [24,25]. CAPP can provide the visual surgical simulation and optimal operation scheme for the surgeons, which saves operation time, minimizes the surgical risks, and improves clinical outcomes [26–28].

Therefore, the purpose of the present study was to investigate the method of application and effect of CAPP on the bridge crane technique for treatment of thoracic ossification of the ligamentum flavum.

Material and Methods

Patient population

A retrospective, multi-center study of patients who underwent the bridge crane technique for TOLF was conducted in 3 hospitals (Shanghai Changzheng Hospital, Ningbo No. 906 Hospital of the People' Liberation Army, and Guangzhou General Hospital of Guangzhou Military Command) from March 2016 to December 2018. The diagnosis of TOLF was based on clinical signs, symptoms, and preoperative computed tomography (CT) scanning. Patients underwent scanning with 1-mm slice thickness (Siemens 64-Slice CT Scanner, Germany). The inclusion criteria were: (1) Thoracic myelopathy and (2) TOLF. The exclusion criteria were: (1) thoracic ossification of the posterior longitudinal ligament (OPLL) (2) spinal surgery, trauma, tumor, deformity, or infection, and (3) incomplete follow-up data. After filtering, 40 patients were enrolled in the study and were divided into Group A (with CAPP, n=21) and Group B (without CAPP, n=19). This study was conducted with approval from the Ethics Committee of our hospital. Written informed consent was obtained from all participants.

Establishment of 3D model

The preoperative scanning data of these patients were saved as Digital Imaging and Communications in Medicine (DICOM) files. The DICOM files of these patients were imported into MIMICS Medical 19.0 software (Materialise, Inc., Belgium) [29]. The operating procedures of establishing the spine 3D model are presented in Figure 1A and were as follow: (1) A bone mask was created by setting a thresholding of bone (226-2998 Hounsfield Unit (HU)). (2) The required region (T8–T12) of the bone mask was selected by pressing the Crop mask button. (3) According to the CT value and anatomy, the selected mask (T8–T12) was revised further by pressing the Edit mask button. (4) The mask of spine (T8–T12) was obtained, and then the mask of TOLF

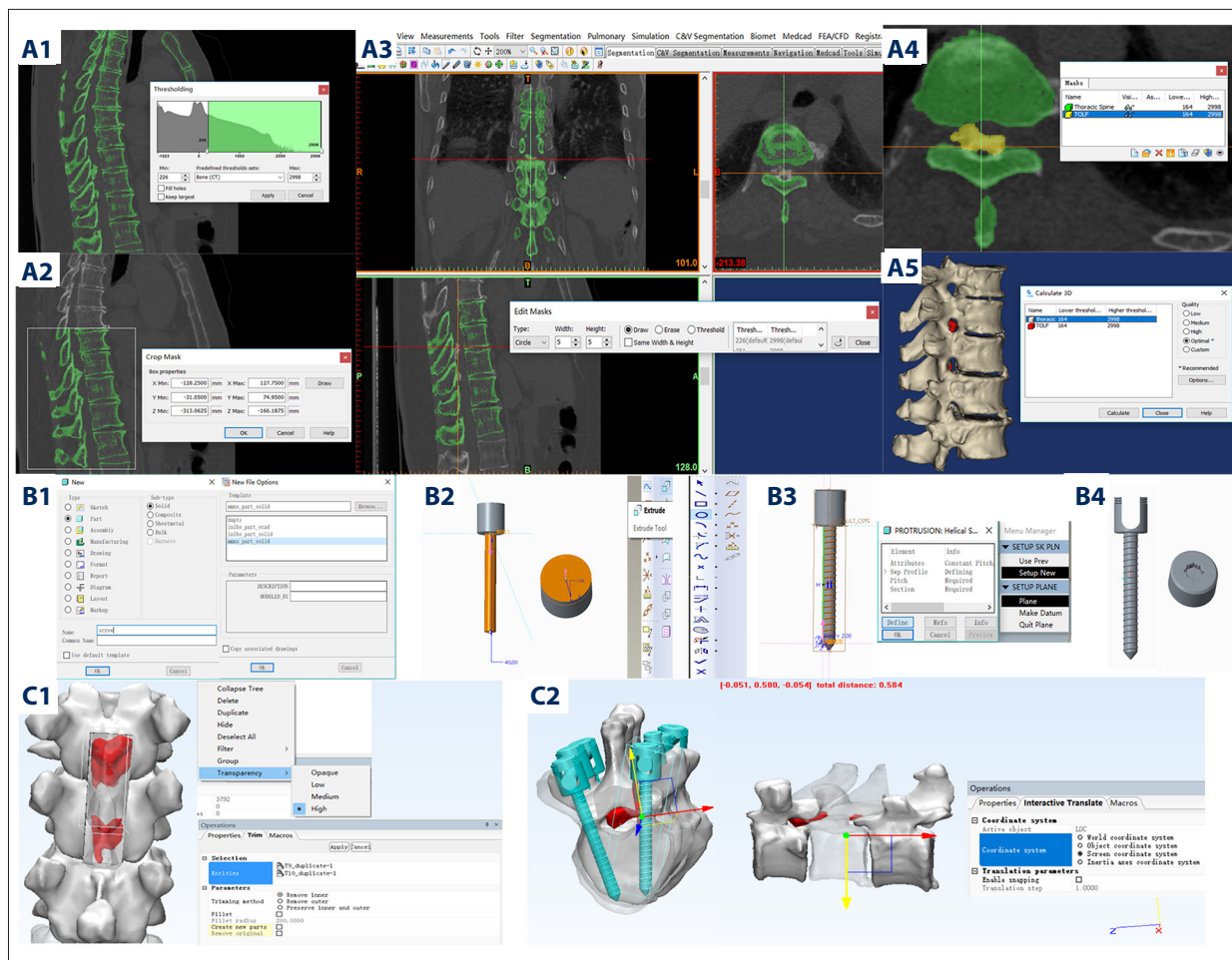


Figure 1. Illustration of the operating procedures of CAPP. The basic operations of establishing the spine 3D model by using MIMICS software (A). Creating a bone mask: press Thresholding button (A1). Selecting the required region: press Crop mask button (A2). Revising the mask: press Edit mask button (A3). Obtaining the revised masks of spine (green) and TOLF (yellow) (A4). Creating the 3D objects of spine and TOLF: press Calculate 3D button (A5). The basic operations of establishing the surgical instrument 3D model by using Pro/Engineer software (B). Entering the specified mode: press mmns_part_solid button (B1). Creating the geometry: use Extrude tool and Geometric tool (B2). Inserting the screw threads: press Protusion button (B3). Obtaining the screws and nuts (B4). The basic operations of virtual surgery by using 3-matic software (C). Visualizing the spine: press Transparency button; Excising the spinal processes: press Trim button (C1). Placing the pedicle screws and moving the LOC: press Interactive Translate button (C2). CAPP – computer-aided preoperative planning; LOC – laminae-OLF complex.

was obtained by using the same method. (5) The obtained spine mask (T8-12 and TOLF) was converted into a 3D object by pressing the Calculate 3D button. (6) The spine 3D model was saved as Stereolithography (STL) files.

The pedicle screws, nuts, longitudinal rods, and transverse connectors were reconstructed in Pro/Engineer 5.0 software (PTC, Inc., USA) [30]. The operating procedures of establishing the surgical instrument 3D model are shown in Figure 1B and were as follows: (1) A specified mode named mmns_part_solid was opened. (2) By using the Extrude and Geometric tool, the surgical instruments were drawn according to their real shape and size, and the screw threads were inserted into the pedicle

screw by pressing the Protusion button. (3) The obtained surgical instrument 3D model was saved as STL files.

Finally, the STL files of thoracic spine and surgical instruments were imported into 3-matic Medical 11.0 software (Materialise, Inc., Belgium) for subsequent use in virtual surgery [31].

Surgical simulation

The virtual surgery was performed in 3-matic Medical 11.0 software. Visualizing, excising, and moving were the main operations of the virtual surgery, which were realized by sequentially

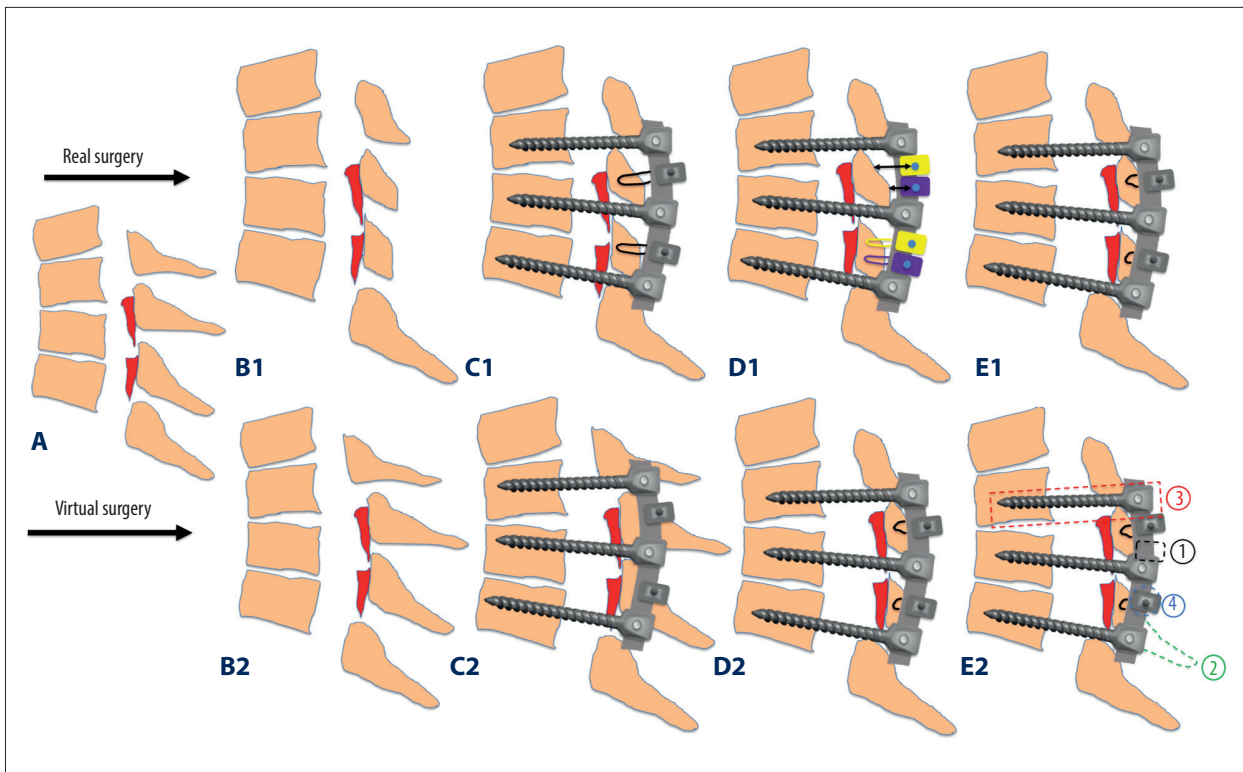


Figure 2. Illustration of the surgical procedures of the bridge crane technique. The sagittal plane of thoracic spine with TOLF (A). Surgical procedures in real surgery (B1, C1, E1): The excision of spinous processes and isolation of the LOC (B1). The installation of the pedicle screws, longitudinal rods, and transverse connectors (C1). The posterior suspension of the LOC (E1). Surgical procedures in virtual surgery (B2–E2): The isolation and posterior suspension of the LOC (B2). The installation of the pedicle screws, longitudinal rods, and transverse connectors (C2). The excision of spinous processes (D2). Adjustment of the parameters in a specific order: 1. the position of the transverse connectors 2. the amount of excision of the spinal processes 3. the length of pedicle screws outside the bone 4. the curvature of the transverse connectors (E2). The different position of transverse connectors: the different distance between LOC and transverse connectors (D1). TOLF – thoracic ossification of the ligamentum flavum; LOC – laminae-OLF complex.

pressing the Transparency, Trim, and Interactive Translate buttons (Figure 1C).

The procedures of the bridge crane technique in virtual surgery were different from those in real surgery (Figure 2A, 2B2–2D2). Firstly, the transparency of the 3D model was increased to make the ossified mass visible in the coronal plane (Figure 3A, 3B). According to the size and shape of the ossified mass, the LOC was safely isolated. Secondly, the LOC was suspended posteriorly based on the evaluation of spinal canal stenosis (Figure 3C). Thirdly, the physiological curvature of the thoracic spine was measured in the sagittal plane. Two longitudinal rods were bent with a similar curvature. The pedicle screws were placed in the bone as deeply as possible and their length outside the bone was not retained. The rods were installed on pedicle screws, and zero-curvature transverse connectors were installed on the rods (Figure 3D). Then, the spinal processes of the involved laminae were excised and sutures were buried at the base of the LOC (Figure 3E).

Finally, if the values of these parameters were not in the appropriate range or could not meet the demand for complete decompression, they would be adjusted in a specific order until satisfactory data were obtained (Figure 2E2). Firstly, changing the position of the transverse connectors could increase the distance between the LOC and transverse connectors (Figure 2D1, Figure 4E). Secondly, if satisfactory decompression was not yet met, the amount of excision of the spinal processes would be increased to enlarge the extent of posterior suspension. Thirdly, the length of pedicle screws outside the bone were retained appropriately. The curvature of the longitudinal rods should also be adjusted for adaption to the screw grooves according to the changed length of all the pedicle screws outside the bone at each level. Finally, the curvature of the transverse connectors was also increased if the previous steps did not work.

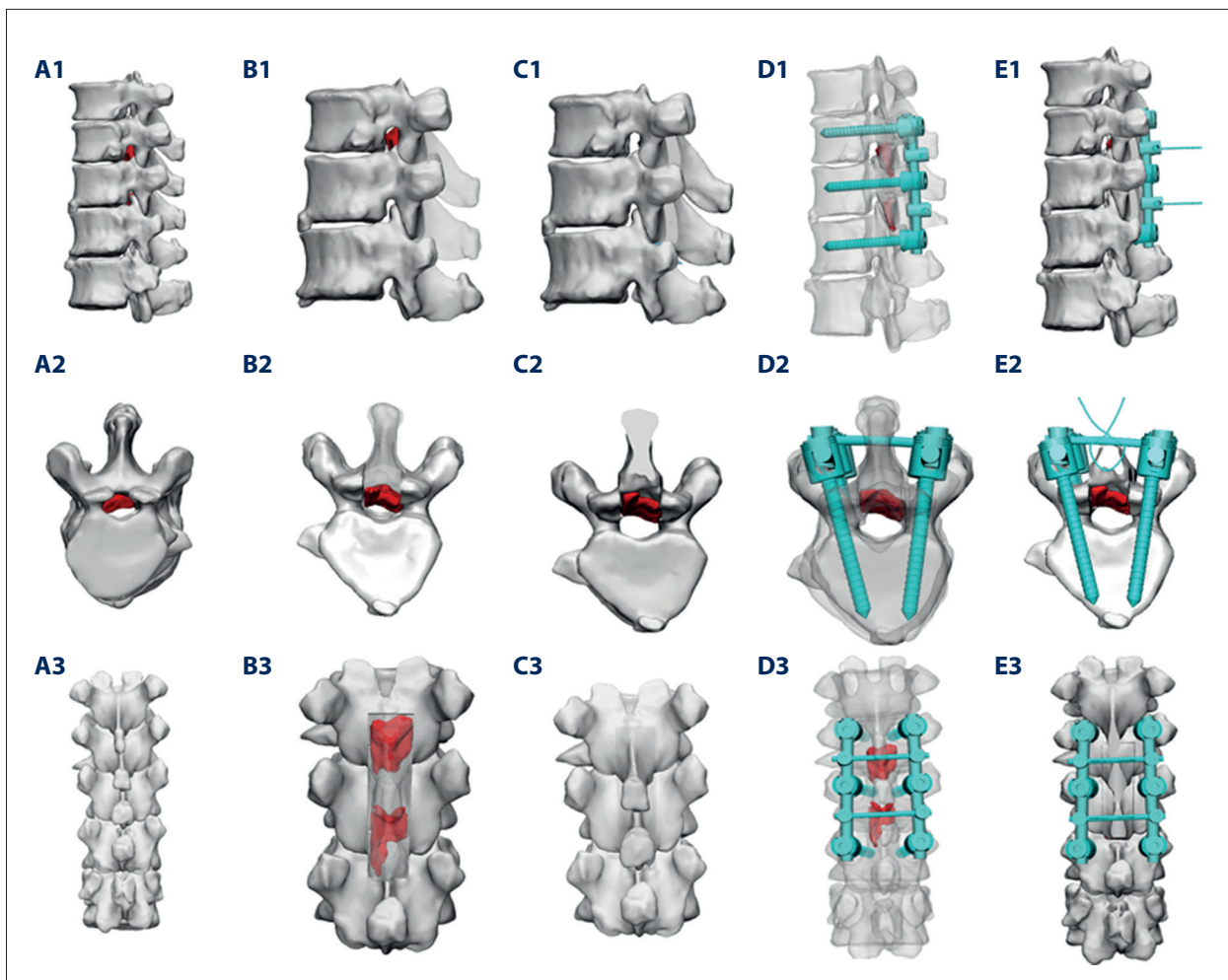


Figure 3. Illustration of the procedures of the bridge crane technique in virtual surgery. The sagittal plane (A1), axial plane (A2), coronal plane (A3) of 3D model (T8–T12). The isolation of the LOC (B1–B3). The posterior suspension of the LOC (C1–C3). The installation of the pedicle screws, longitudinal rods and transverse connectors (D1–D3). The excision of spinous processes (E1–E3). LOC – laminae-OLF complex.

Intraoperative application

During the actual surgery, the spinal processes were first excised according to the amount of excision in CAPP (Figure 2B1). Then, the positioning screws were placed into the pedicles. By using the positioning screws as a reference, the range of LOC isolation was determined according to the preoperative width and length of the LOC. The positioning screws were removed and the pedicle screws were placed according to the preoperative length outside the bone. Two longitudinal rods and the transverse connectors were bent with a planned curvature. The planned positions of the transverse connectors installed on the rods were marked, and then the longitudinal rods and the transverse connectors were installed on the pedicle screws successively, which were fixed by nuts (Figure 2C1). Finally, the sutures were tied to the transverse connectors and the LOC was successfully suspended (Figure 2E1). The caliper

and specially-made curvature ruler were used for parameter measurement to ensure that the operation was performed according to the preoperative plan [32].

Clinical assessment

The patients' preoperative and postoperative neurological function were assessed by a modified Japanese Orthopaedic Association (mJOA) scoring system for thoracic myelopathy [33], as shown in Table 1. Recovery rate (RR) represented recovery degree of neurological function as follows: $RR = (\text{postoperative JOA score} - \text{preoperative JOA score}) / (11 - \text{preoperative JOA score}) \times 100\%$. The criteria for surgical outcomes was defined as follows: Excellent $\geq 75\%$, 74% \geq Good $\geq 50\%$, 49% \geq Fair $\geq 25\%$, and 24% \geq Poor $\geq 0\%$. The postoperative mJOA scores of these patients were calculated at the last follow-up. The follow-up period of all the patients was not less than 6 months. The surgical

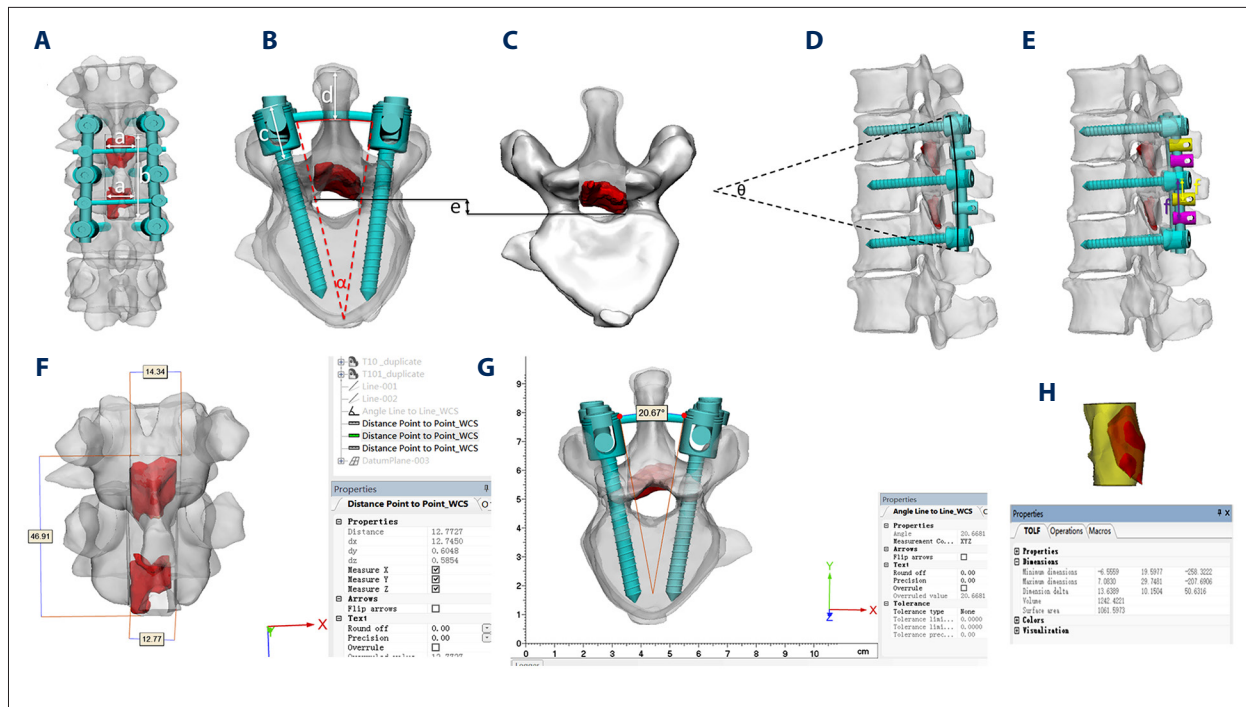


Figure 4. Illustration of the anatomical parameters. a=Width of LOC, b=Length of LOC (A). c=Length of pedicle screws outside the bone, d=Amount of excision of the spinal processes, e=Height of posterior suspension of LOC, α =Curvature of the transverse connectors (B, C). θ =Curvature of the longitudinal rods (D). f=Position of the transverse connectors (distance between the cranial neighboring pedicle screw and the transverse connector) (E). The distance measurement: press Distance Point to Point_WCS button (F). The curvature measurement: press Angle Line to Line_WCS button (G). The volume measurement (spinal canal volume (yellow) and TOLF volume (red)): press Dimensions button (H). TOLF – thoracic ossification of the ligamentum flavum; LOC – laminae-OLF complex.

complications including residual ossified lesion, CSF leakage, neurologic deterioration, and instrumentation-related complications were also recorded.

Radiological assessment

The degree of spinal canal stenosis was assessed by measuring the spinal volume occupation ratio (SVOR) and spinal volume recovery rate (SVRR) [34]. The SVOR and SVRR were measured by using 3-matic software (Figure 4H). SVOR was calculated as: TOLF volume within spinal canal/spinal canal volume \times 100%. SVRR was calculated as: SVRR=preoperative SVOR–postoperative SVOR. All the radiological methods, including plain radiographs, CT, and MRI, were conducted within 3 days after surgery and at the final follow-up period.

The 8 anatomical parameters – the length and width of LOC, the length of pedicle screws outside the bone, the amount of excision of the spinal processes, the height of posterior suspension of the LOC, the curvature of the transverse connectors, the curvature of the longitudinal rods, and the position of the transverse connectors – were measured in the preoperative 3D model and postoperative CT images, as shown in Figure 4.

To ensure that the intra-observer and inter-observer reliability for radiological assessment was acceptable, 2 independent reviewers measured all the parameters 3 times and calculated their mean values.

Statistical analysis

Statistical data were analyzed using SPSS (version 19.0, SPSS, Inc., Chicago, IL, USA). The results were reported as mean \pm SD (mean \pm standard deviation). The independent-samples *t* test was used to compare clinical and radiological outcomes between Group A and Group B. The Pearson's chi-square test was used in the comparisons of sex, TOLF type, RR grade, and complications between Group A and Group B. The paired *t* test was used to compare the anatomical parameters between preoperative simulation and postoperative CT, or postoperative CT and postoperative simulation. *p*<0.05 was defined as a significant difference.

Results

Table 2 demonstrates the demographic data of patients with TOLF. A total of 40 patients who underwent the bridge crane

Table 1. Modified Japanese Orthopaedic Association (mJOA) scoring system for the assessment of thoracic myelopathy.

Categories	Score (points)
<i>Motor function: lower extremity</i>	
Impossible to walk	0
Need a cane or aid on flat ground	1
Need aid only on stairs	2
Possible to walk without any aid, but slow manner	3
Normal	4
<i>Sensory function: lower extremity</i>	
Apparent sensory disturbance	0
Minimal sensory disturbance	1
Normal	2
<i>Sensory function: Trunk</i>	
Apparent sensory disturbance	0
Minimal sensory disturbance	1
Normal	2
<i>Bladder function</i>	
Urinary retention or incontinence	0
Severe dysuria (sense of retention, staining)	1
Slight dysuria (pollakisuria, retardation)	2
Normal	3
<i>Total score</i>	11

technique were divided into Group A and Group B. There were 21 patients in Group A and 19 patients in Group B. There was no significant difference in preoperative data, including sex, age, symptom duration, follow-up, TOLF extent, and TOLF type, between the 2 groups ($p>0.05$).

Table 2. Characteristic features of the patients with TOLF in 2 groups.

	Group A (n=21)	Group B (n=19)	P value
Sex (Male/Female)	14/7	11/8	0.57
Age (year)	51.8±11.1	54.6±9.8	0.40
Symptom duration (month)	20.1±10.9	18.3±12.6	0.63
Follow-up (month)	10.2±4.2	11.6±4.7	0.33
TOLF extent (segment)	3.2±1.1	3.4±1.2	0.53
TOLF type on axial CT (lateral/enlarged/fused/tuberous)	0/7/9/5	1/5/11/2	0.46
TOLF type on sagittal CT (continuous/noncontinuous)	19/2	15/4	0.56

* Difference was defined as significant when $p<0.05$. The results were reported as mean±SD (mean±standard deviation).
TOLF – thoracic ossification of the ligamentum flavum.

Clinical outcomes

As shown in Table 3, the mean total time for CAPP was 84±25 min (range, 50–125 min). The mean time for establishing the spine 3D model was 46.0±11 min (range, 25–65 min). The mean time for establishing the surgical instrument 3D model was 29±6 min (range, 25–40 min). The mean time for virtual surgery was 27±10 min (range, 15–35 min).

There was no significant difference in blood loss between the 2 groups ($p>0.05$). However, shorter operation time and fewer fluoroscopic images were obtained in Group A than in Group B (185±29 min vs. 211±42 min, $p<0.05$; 3.3±0.8 vs. 6.1±1.2, $p<0.01$). There was no significant difference in pre-mJOA and pre-SVOR scores between the 2 groups ($p>0.05$).

The mean postoperative mJOA scores in both groups had all increased substantially at final follow-up, and patients in Group A had higher mJOA scores (8.8±1.8 vs. 7.3±2.4) and RR of neurological function (65.7±21.4% vs. 48.2±30.6%) than those in Group B ($p<0.05$). The distribution of RR grade in Groups A and B was 8/6 for excellent, 9/4 for good, 3/6 for fair, and 1/3 for poor, respectively.

A total of 7 patients had complications, including residual ossified lesion (0 in Group A and 2 in Group B), CSF leakage (1 in Group A and 3 in Group B), and neurologic deterioration (0 in Group A and 1 in Group B). No instrumentation-related complications were observed in either group. The incidence of complications in Group A was lower than in Group B, but the difference was not significant ($p=0.07$).

Radiological outcomes

There was no significant difference in post-SVOR and SVRR scores between the 2 groups ($p>0.05$).

Table 3. Comparison of clinical and radiological outcomes between 2 groups.

	Group A	Group B	P value
Pre-planning time (minutes)	84±25	NA	NA
Operative time (minutes)	185±29	211±42	0.03*
Blood loss (ml)	532±83	515±124	0.61
No. of fluoroscopies	3.3±0.8	6.1±1.2	<0.01*
Pre-mJOA	5.2±1.9	4.7±2.0	0.41
Post-mJOA (Final visit)	8.8±1.8	7.3±2.4	0.04*
RR	65.7±21.4	48.2±30.6	0.04*
RR grade (excellent/good/fair/poor)	8/9/3/1	6/4/6/3	0.29
Pre-SVOR	13.8±6.0 (4.8–27.9)	15.7±6.7 (6.6–31.1)	0.33
Post-SVOR	1.1±2.6 (–3.9–4.9)	1.7±4.9 (–6.2–8.5)	0.61
SVRR	12.7±6.3 (3.3–24.7)	14.1±5.1 (5.2–22.6)	0.46
Complications	1 (4.8%)	6 (31.6%)	0.07
Residual ossified lesion	0	2	
CSF leakage	1	3	
Neurologic deterioration	0	1	
Instrumentation-related complications	0	0	

* Difference was defined as significant when $p < 0.05$. The results were reported as mean±SD (mean±standard deviation). NA – not applicable; mJOA – modified Japanese Orthopaedic Association; RR – recovery rate; SVOR – spinal volume occupation ratio; SVRR – spinal volume recovery rate; CSF leakage – cerebrospinal fluid leakage.

Table 4. Comparison of preoperative and postoperative anatomical parameters in Group A.

Anatomical parameters	Preoperative	Postoperative	t Value (P)
Width of LOC (mm)	17.8±2.5 (12.8–22.4)	17.9±2.5 (13.1–21.5)	0.64
Length of LOC (mm)	55.4±14.5 (33.7–79.8)	55.8±13.3 (35.6–77.5)	0.40
Length of pedicle screws outside the bone (mm)	17.3±1.9 (14.5–20.0)	17.2±1.6 (14.5–19.1)	0.55
Amount of excision of the spinal processes (mm)	7.1±1.4 (5.0–9.4)	7.0±1.3 (5.8–9.3)	0.54
Position of the transverse connectors (mm)	12.9±2.9 (6.2–17.0)	13.0±2.7 (7.5–16.6)	0.62
Height of posterior suspension of LOC (mm)	7.3±1.4 (4.5–9.1)	7.4±1.4 (4.7–9.4)	0.22
Curvature of the longitudinal rods (°)	8.8±5.7 (0.0–16.0)	8.9±5.9 (0.0–17.3)	0.74
Curvature of the transverse connectors (°)	14.5±10.9 (0.0–30.0)	14.0±10.9 (0.0–33.3)	0.15

The results were reported as mean±SD (mean±standard deviation). LOC – laminae-OLF complex.

In the 21 patients in Group A, the anatomical parameters of preoperative design and postoperative CT were compared. There was a high consistency in width and length of the LOC, length of pedicle screws outside the bone, amount of excision of the spinal processes, position of the transverse connectors, height of posterior suspension of LOC, curvature of the longitudinal rods, and curvature of the transverse connectors before and after surgery, as shown in Table 4 ($p > 0.05$).

We performed 3D simulation and surgical design postoperatively for the 19 patients in Group B. The anatomical parameters of postoperative simulation and postoperative CT measurement were compared, as shown in Table 5. There were no significant differences in width of LOC, length of the LOC, position of transverse connectors, height of posterior suspension of the LOC, and curvature of longitudinal rods between postoperative simulation and postoperative CT ($p > 0.05$). However, there were statistically significant differences in the

Table 5. Comparison of the anatomical parameters regarding postoperative simulation and postoperative CT in Group B.

Anatomical parameters	Postoperative simulation	Postoperative CT	t Value (P)
Width of LOC (mm)	19.4±2.5 (15.2–23.8)	19.2±2.8 (13.1–24.0)	0.58
Length of LOC (mm)	53.8±14.5 (36.0–82.7)	55.4±14.2 (39.6–82.1)	0.07
Length of pedicle screws outside the bone (mm)	17.9±1.7 (14.5–20.5)	16.5±1.7 (14.5–20.4)	0.01*
Amount of excision of the spinal processes (mm)	7.6±1.5 (5.0–10.4)	8.7±1.7 (6.0–12.4)	0.02*
Position of the transverse connectors (mm)	9.4±2.6 (6.5–15.2)	10.2±2.2 (6.5–14.6)	0.30
Height of posterior suspension of LOC (mm)	7.5±1.3 (5.0–9.5)	7.2±1.5 (4.4–9.8)	0.39
Curvature of the longitudinal rods (°)	11.5±6.2 (0.0–19.6)	13.6±6.9 (0.0–22.9)	0.24
Curvature of the transverse connectors (°)	17.2±9.5 (0.0–30.0)	9.4±7.9 (0.0–24.8)	0.02*

* Difference was defined as significant when $p < 0.05$. The results were reported as mean±SD (mean±standard deviation).
LOC – laminae-OLF complex.

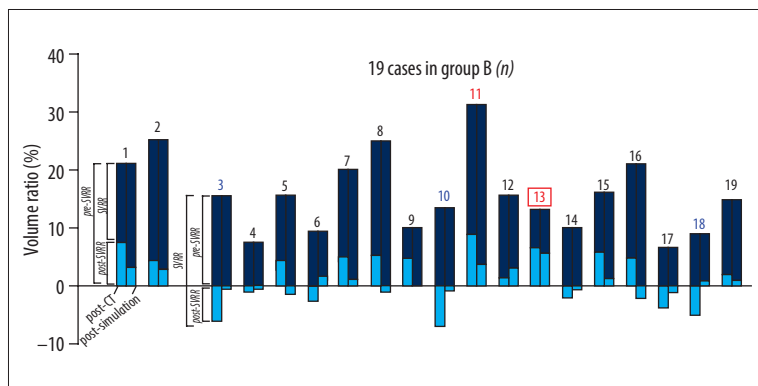


Figure 5. Illustration of the radiological parameters of 19 patients in postoperative simulation and postoperative CT. The black number indicates the patients with no complication, the red number indicates the patients with residual ossified lesion, the blue number indicates the patients with CSF leakage and “□” indicated the patients with neurologic deterioration. CSF leakage: Cerebrospinal fluid leakage.

Table 6. Comparison of the radiological parameters regarding the decompression effect between postoperative simulation and postoperative CT in Group B (the patients with no complications, n=14).

Radiological parameters	Postoperative simulation	Postoperative CT	t Value (P)
Post-SVOR	0.3±1.8 (-2.2–3.1)	2.5±3.6 (-3.8–7.4)	0.03*
SVRR	15.2±5.9 (7.1–26.0)	13.0±4.1 (5.2–20.7)	0.03*
Height of posterior suspension of LOC (mm)	7.4±1.3 (5.0–9.5)	6.9±1.0 (5.0–8.8)	0.04*

* Difference was defined as significant when $p < 0.05$. The results were reported as mean± SD (mean±standard deviation).
SVOR – spinal volume occupation ratio; SVRR – spinal volume recovery rate; LOC – laminae-OLF complex.

length of pedicle screws outside the bone (17.9±1.7 mm vs. 16.5±1.7 mm), amount of excision of spinal processes (7.6±1.5 mm vs. 8.7±1.7 mm), and curvature of the transverse connectors (17.2±9.5° vs. 9.4±7.9°) between postoperative simulation and postoperative CT ($p < 0.05$).

(2.5±3.6 mm vs. 0.3±1.8 mm), lower SVRR scores (13.0±4.1 mm vs. 15.2±5.9 mm), and height of posterior suspension of LOC (6.9±1.0 mm vs. 7.4±1.3 mm) in postoperative CT than those in postoperative simulation ($p < 0.05$), as shown in Table 6.

The detailed radiological data from postoperative simulation and postoperative CT in Group B are shown in Figure 5. Of note, after exclusion of patients with complications in Group B, those with no complications had higher post-SVOR scores

Discussion

Thoracic ossification of the ligamentum flavum (TOLF) was first reported by Polgar in 1920 [35]. Its main feature is ectopic

osteogenesis of the thoracic ligamentum flavum, which leads to compression of the thoracic spinal cord. TOLF has gradually become the primary cause of thoracic myelopathy for East Asian people, especially for Japanese, and whites [36]. Once this disease is diagnosed, surgical decompression is generally considered the most effective treatment. The current surgical treatment methods include laminectomy and fenestration. Nevertheless, these methods usually need to invade the spinal canal and remove the ossified mass directly, which can damage the spinal cord [37]. The high risk of early complications such as neurological deficits and cerebrospinal fluid (CSF) leakage are also why it is hard to achieve satisfactory clinical outcomes using these surgical methods [6–9].

To reduce the risk of complications and improve the safety of surgical procedures, a novel surgical technique named the bridge crane technique has been used to treat severe TOLF [10]. The idea of the surgical technique is to isolate and suspend the TOLF with the help of the instrument, similar to lifting material vertically with the help of a bridge crane machine when building a bridge. This surgical method to restore the original volume of the spinal canal by suspending instead of resecting the TOLF can avoid invading the spinal canal and damaging the spinal cord. The reconstruction of the remaining laminae and TOLF as autologous bones can continue to maintain the stability of the thoracic spine.

The key procedure of the bridge crane technique is longitudinal and transverse osteotomy, and posterior suspension of the isolated TOLF. The range of longitudinal and transverse osteotomy (width and length of the laminae-OLF complex (LOC)) determines whether the TOLF can be isolated completely, and the decompression effect depends on the distance of posterior suspension of isolated LOC (the combination of 4 parameters). Any inappropriate value or combination of the parameters can increase the risk of complications. In Group B (without CAPP), 2 major complications were observed. Firstly, 2 patients with residual ossified lesion were observed to have an insufficient width of the LOC. One of these 2 patients also experienced neurological deterioration. TOLF often originates from the bilateral vertebral and articular processes, so LOC insufficient width is like to cause a residual ossified lesion [38]. Secondly, 3 patients with CSF leakage were observed. Their postoperative SVOR were -6.2% , -7.0% , and -5.1% . Considering that TOLF often adheres to the dura mater and even causes dural ossification, we suspected that excessive posterior suspension had led to dural tearing and CSF leakage [15].

Due to the invisible surgical procedure, complete isolation and precise posterior suspension can be a challenge for surgeons. To solve the above problems as much as possible, computer-aided design (CAD) was used in our preoperative planning. With the help of 3 different types of CAD software we formulated

an efficient and feasible process of CAPP and its intraoperative application for the bridge crane technique. In the process, the 3D models of thoracic spine and surgical instruments were reconstructed by using MIMICS and Pro/Engineer software based on the actual CT data and physical data. The precision of reconstruction has been widely recognized and has been reported in previous studies [39,40]. Then, the transparency of the spine model was increased and TOLF hidden in the spinal canal was revealed. The visualization of the 3D model can help surgeons precisely position and isolate the ossified mass completely. Furthermore, surgeons can also change the surgical sequence to obtain an optimal planning for precise posterior suspension. In practice, the distance of posterior suspension of isolated LOC is easily determined according to the thickness of the TOLF, but the amount of excision of spinal processes is difficult to determine at first. In actual surgery, the surgeons can only estimate the amount of excision of spinal processes based on experience and then roughly evaluate the decompression effect by reduplicated fluoroscopy, which can increase the surgical risks and radiation exposure of patients. In virtual surgery, surgeons can easily determine the suspension distance and then adjust other parameters based on the suspension situation. In addition, the specially-made measurement tools and intraoperative procedure can help surgeons perform the operation accurately according to the preoperative planning. We compared the main parameters in preoperative planning with those in postoperative CT and found there was a high consistency of the 8 main parameters ($p>0.05$), which demonstrated that the effectiveness and reliability of the CAPP process and its intraoperative application. In fact, the accuracy and reliability of the similar process of CAPP from the preoperative planning to the real-time operation has been proved in other research [41–44]. The mean (SD) errors of the most commonly observed parameters between preoperative planning and postoperative CT were small and acceptable in these studies. Of note, significant differences between preoperative planning and postoperative CT were observed only in some deformable parameters such as the intercondylar distance and height of the intervertebral space in these studies. The error in intercondylar distance was caused by the pull of muscles, and the error in the height of intervertebral space was caused by the difference in body position, so these influencing factors should be considered in planning. Since the parameters involved in our study were rigid or bony, the impact of these factors was minimal.

To further explore the utility and effect of CAPP, the clinical outcomes of the 2 groups were compared. As the results show, the patients in Group A obtained higher mJOA scores and RR of neurological function than those in Group B ($p<0.05$). The following 2 factors might have contributed to the above results. Firstly, the incidence of complications in Group A was far lower than in Group B (4.8% vs. 31.6%). Secondly, incomplete decompression

might have occurred in some patients in Group B. Spinal volume parameters about such as SVOR and SVVR are the most important indicators for prognosis of decompression surgery [34,45]. After exclusion of patients with complications in Group B, those with no complications obtained higher post-SVOR and lower SVRR and height of posterior suspension of LOC in postoperative CT than those in postoperative simulation ($p < 0.05$). This demonstrated that complete TOLF isolation and precise posterior suspension were achieved with the aid of CAPP, which minimized the risks of incomplete decompression, CSF leakage (excessive decompression), and residual ossified lesions. In addition, Group A had shorter operation time and fewer fluoroscopic images than Group B ($p < 0.05$). We also found that CAPP can help surgeons minimize operation time by avoiding repeated intraoperative attempts and operations, including bending the rods, performing fluoroscopy, and adjustment of other parameters, as well as minimizing radiation exposure of patients.

We also found that there were statistically significant differences in some anatomical parameters between postoperative simulation and postoperative CT in Group B ($p < 0.05$). As the results showed, the spinal decompression was achieved by a larger amount of excision of the spinal processes instead of increasing the length of pedicle screws outside the bone and curvature of the transverse connectors. In many cases, it was insufficient to rely solely on the amount of excision of the spinal processes. Therefore, more parameters need to be involved in the operation for complete decompression. In clinical practice, it is difficult for surgeons to control the length of pedicle screws outside the bone and curvature of the transverse connectors during surgery. However, our research has solved the critical clinical problem. The precise and controllable multi-parameter-related decompression can be achieved by quantitative preoperative planning.

One of the CAPP technologies – computer-aided virtual surgery technology – was used in our study. Currently, virtual surgery and 3D-printing technologies are the main means utilized for preoperative planning [20]. Their advantages, including better clinical outcomes, less blood loss, shorter operation time, and fewer fluoroscopic images, were reported in the previous studies, most of which were also presented in the present report [46,47]. Compared with 3D-printing technology, the advantages of virtual surgery technology lie in more convenient surgical simulation, less preoperative planning time, shorter hospital stay, and no extra cost [47]. However, dealing with

the 3D images by the 2D method (using the mouse) is its biggest shortcoming. Conversely, 3D-printing technology can provide a physical model for the surgeon to perform anatomical operations, which is more similar to the real surgery [48]. In recent years, some novel technologies such as virtual reality (VR) and mixed reality (MR) have developed and are already used in preoperative planning. VR technology lacks the shortcoming of virtual surgery technology and enables the surgeon to obtain surgical experience similar to the real physical environment by using 3D interactive devices, but if fails to give the surgeon a “real-touch” experience [49,50]. As an improvement of VR technology, MR technology can combine the virtual surgery with the perception of the real environment, such as vision and touch, which provides an almost real surgical experience [51,52]. However, whether VR and MR technologies can improve surgical results and patient outcomes needs to be confirmed [49].

The present study has certain limitations. Firstly, the sample size was not large enough and we speculated that this was the main reason for finding no statistically significant difference in complications between the 2 groups. Secondly, the follow-up time was too short, which might be why we observed no instrumentation-related complications. Thirdly, CAPP requires the surgeons to have computer skills or spend time mastering these skills, which might be a challenge for some surgeons. Finally, the bridge crane technique is a novel treatment approach for TOLF, and its long-term follow-up outcomes have not been reported yet. Therefore, the clinical value and advantages of the surgical technique need further evaluation, although we have presented some clinical outcomes here.

Conclusions

The process of CAPP and its intraoperative application for the bridge crane technique are reliable and feasible. CAPP can enable surgeons to control the decompression effect accurately and reduce the risk of related complications, which improves the safety and efficacy of the bridge crane technique for the treatment of TOLF. Nevertheless, studies with more patients and longer follow-up are needed to further prove the effectiveness of CAPP and the bridge crane technique itself.

Conflict of interest.

None.

References:

1. Wang B, Chen Z, Meng X et al: iTRAQ quantitative proteomic study in patients with thoracic ossification of the ligamentum flavum. *Biochem Biophys Res Commun*, 2017; 487(4): 834–39
2. Zhou SY, Yuan B, Qian C et al: Evaluation of measuring methods of spinal canal occupation rate in thoracic ossification of ligamentum flavum. *World Neurosurg*, 2018; 110: e1025–30
3. Feng FB, Sun CG, Chen ZQ: Progress on clinical characteristics and identification of location of thoracic ossification of the ligamentum flavum. *Orthop Surg*, 2015; 7(2): 87–96
4. Zhang J, Wang L, Li J et al: Predictors of surgical outcome in thoracic ossification of the ligamentum flavum: Focusing on the quantitative signal intensity. *Eur Sci Rep*, 2016; 6: 23019
5. Miao X, He D, Wu T, Cheng X: Percutaneous endoscopic spine minimal invasive technique for the decompression therapy of thoracic myelopathy caused by ossification of the ligamentum flavum. *World Neurosurg*, 2018; 114: 8–12
6. Miyashita T, Ataka H, Tanno T: Spontaneous reduction of a floated ossification of the ligamentum flavum after posterior thoracic decompression (floating method); Report of a case (abridged translation of a primary publication). *Spine J*, 2013; 13(8): e7–9
7. Osman NS, Cheung ZB, Hussain AK et al: Outcomes and complications following laminectomy alone for thoracic myelopathy due to ossified ligamentum flavum. *Spine*, 2018; 43(14): E842–48
8. Tang CYK, Cheung JPY, Samartzis D et al: Predictive factors for neurological deterioration after surgical decompression for thoracic ossified yellow ligament. *Eur Spine J*, 2017; 26(10): 2598–605
9. Li B, Qiu G, Guo S et al: Dural ossification associated with ossification of ligamentum flavum in the thoracic spine: a retrospective analysis. *BMJ Open*, 2016; 6(12): e013887
10. Jingchuan S, Kaiqiang S, Jiangang S et al: The bridge crane technique for the treatment of the severe thoracic ossification of the ligamentum flavum with myelopathy. *Eur Spine J*, 2018; 27(8): 1846–55
11. Kanno H, Takahashi T, Aizawa T et al: Recurrence of ossification of ligamentum flavum at the same intervertebral level in the thoracic spine: A report of 2 cases and review of the literature. *Eur Spine J*, 2017; 27(Suppl. 3): 359–67
12. Barath AS, Wu OC, Patel M, Kasliwal MK: Repeated recurrence of thoracic spine stenosis following decompression alone for ossification of the ligamentum flavum: Case report. *J Neurosurg Spine*, 2018; 30(3): 332–36
13. Sun J, Xu X, Wang Y et al: How to avoid postoperative remaining ossification mass in anterior controllable antedisplacement and fusion surgery. *World Neurosurg*, 2019; 3: 100034
14. Aizawa T, Sato T, Ozawa H et al: Sagittal alignment changes after thoracic laminectomy in adults. *J Neurosurg Spine*, 2008; 8(6): 510–16
15. Hou X, Chen Z, Sun C et al: A systematic review of complications in thoracic spine surgery for ossification of ligamentum flavum. *Spinal Cord*, 2017; 56(4): 301–7
16. Hermansen E, Moen G, Fenstad AM et al: Spinous process osteotomy to facilitate the access to the spinal canal when decompressing the spinal canal in patients with lumbar spinal stenosis. *Asian Spine J*, 2014; 8(2): 138–44
17. Li M, Wang Z, Du J et al: Thoracic myelopathy caused by ossification of the ligamentum flavum a retrospective study in Chinese patients. *J Spinal Disord Tech*, 2013; 26(1): E35–40
18. Yang JS, Sponseller PD, Thompson GH et al., Growing Spine Study Group: Growing rod fractures: Risk factors and opportunities for prevention. *Spine*, 2011; 36(20): 1639–44
19. Smith JS, Shaffrey CI, Ames CP et al., International Spine Study Group: Assessment of symptomatic rod fracture after posterior instrumented fusion for adult spinal deformity. *Neurosurgery*, 2012; 71(4): 862–67
20. Zheng YX, Yu DF, Zhao JG et al: 3D Printout models vs. 3D-rendered images: Which is better for preoperative planning? *J Surg Educ*, 2016; 73(3): 518–23
21. Zheng GS, Su YX, Liao GQ et al: Mandible reconstruction assisted by preoperative virtual surgical simulation. *Oral Surg Oral Med Oral Pathol Oral Radiol*, 2012; 113(5): 604–11
22. Mehta MP, Vogel LA, Shiu BB et al: Determining glenoid component version after total shoulder arthroplasty. *J Shoulder Elbow Surg*, 2018; 27(9): 1588–95
23. Yang ML, Zhang B, Zhou Q et al: Minimally-invasive open reduction of intracapsular condylar fractures with preoperative simulation using computer-aided design. *Br J Oral Maxillofac Surg*, 2013; 51(3): e29–33
24. Egger J, Wallner J, Gall M et al: Computer-aided position planning of mini-plates to treat facial bone defects. *PLoS One*, 2017; 12(8): e0182839
25. Polley JW, Figueroa AA: Orthognathic positioning system: Intraoperative system to transfer virtual surgical plan to operating field during orthognathic surgery. *J Oral Maxillofac Surg*, 2013; 71(5): 911–20
26. Chang EI, Jenkins MP, Patel SA, Topham NS: Long-term operative outcomes of preoperative computed tomography-guided virtual surgical planning for osteocutaneous free flap mandible reconstruction. *Plast Reconstr Surg*, 2016; 137(2): 619–23
27. Wang H, Wang F, Newman S et al: Application of an innovative computerized virtual planning system in acetabular fracture surgery: A feasibility study. *Injury*, 2016; 47(8): 1698–701
28. Chen X, Xu L, Sun Y, Politis C: A review of computer-aided oral and maxillofacial surgery: Planning, simulation and navigation. *Expert Rev Med Devices*, 2016; 13(11): 1043–51
29. The Mimics Medical 19.0 software. Available from: URL: <https://www.materialise.com/en/medical/software/mimics>
30. The Pro/Engineer 5.0 software. Available from: URL: <https://www.ptc.com/en/products/cad/pro-engineer>
31. The 3-matic Medical 11.0 software. Available from: URL: <https://www.materialise.com/en/software/3-matic>
32. Sun J, Sun K, Wang Y et al: Quantitative anterior enlargement of the spinal canal by anterior controllable antedisplacement and fusion (ACAF) for the treatment of cervical ossification of the posterior longitudinal ligament with myelopathy. *World Neurosurg*, 2018; 120: e1098–106
33. Zhang JT, Wang LF, Li J et al: Predictors of surgical outcome in thoracic ossification of the ligamentum flavum: Focusing on the quantitative signal intensity. *Sci Rep*, 2016; 6: 23019
34. Lee N, Ji GY, Shin HC et al: Usefulness of 3-dimensional measurement of ossification of the posterior longitudinal ligament (OPLL) in patients with OPLL-induced myelopathy. *Spine*, 2015; 40(19): 1479–86
35. Kim SI, Ha KY, Lee JW, Kim YH: Prevalence and related clinical factors of thoracic ossification of the ligamentum flavum – a computed tomography-based cross-sectional study. *Spine J*, 2017; 18(4): 551–57
36. Ahn DK, Lee S, Moon SH et al: Ossification of the ligamentum flavum. *Asian Spine J*, 2014; 8(1): 89–96
37. Wang CH, Cui WL, Xue JL, Liao Z: Transforaminal en bloc resection for the treatment of thoracic ossification of the ligamentum flavum: Retrospective cohort study. *Int J Surg*, 2018; 54(Pt A): 278–84
38. Zhou S, Yuan B, Qian C et al: Evaluation of measuring methods of spinal canal occupation rate in thoracic ossification of ligamentum flavum. *World Neurosurg*, 2018; 110: e1025–30
39. An G, Hong L, Zhou XB et al: Accuracy and efficiency of computer-aided anatomical analysis using 3D visualization software based on semi-automated and automated segmentations. *Ann Anat*, 2017; 210: 76–83
40. Burkhard JPM, Dietrich AD, Jacobsen C et al: Cephalometric and three-dimensional assessment of the posterior airway space and imaging software reliability analysis before and after orthognathic surgery. *J Craniomaxillofac Surg*, 2014; 42(7): 1428–36
41. Sun H, Li B, Zhao Z et al: Error analysis of a CAD/CAM method for unidirectional mandibular distraction osteogenesis in the treatment of hemifacial microsomia. *Br J Oral Maxillofac Surg*, 2013; 51(8): 892–97
42. Jud L, Müller DA, Fürnstahl P et al: Joint-preserving tumour resection around the knee with allograft reconstruction using three-dimensional preoperative planning and patient-specific instruments. *Knee*, 2019; 26(3): 787–93
43. Sun JC, Sun KQ, Sun SX et al: Computer-assisted virtual operation planning in anterior controllable anterior-displacement and fusion surgery for ossification. *Clin Neurol Neurosurg*, 2019; 177: 86–91
44. Totoki Y, Yoshii Y, Kusakabe T et al: Screw length optimization of a volar locking plate using three dimensional preoperative planning in distal radius fractures. *J Hand Surg Asian Pac Vol*, 2018; 23(4): 520–27
45. Sun K, Wang S, Sun J et al: Analysis of the correlation between cerebrospinal fluid space and outcomes of anterior controllable antedisplacement and fusion for cervical myelopathy due to ossification of the posterior longitudinal ligament. *World Neurosurg*, 2019; 122: e358–66

46. Xue L, Fan H, Shi W et al: Preoperative 3-dimensional computed tomography lung simulation before video-assisted thoracoscopic anatomic segmentectomy for ground glass opacity in lung. *J Thorac Dis*, 2018; 10(12): 6598–605
47. Chen Y, Jia X, Qiang M et al: Computer-assisted virtual surgical technology versus three-dimensional printing technology in preoperative planning for displaced three and four-part fractures of the proximal end of the humerus. *J Bone Joint Surg Am*, 2018; 100(22): 1960–68
48. Smith ML, Mcguinness J, O'Reilly MK et al: The role of 3D printing in preoperative planning for heart transplantation in complex congenital heart disease. *Ir J Med Sci*, 2017; 186(3): 753–56
49. González Sánchez JJ, Enseñat Nora J, Candela Canto S et al: New stereoscopic virtual reality system application to cranial nerve microvascular decompression. *Acta Neurochir (Wien)*, 2010; 152(2): 355–60
50. Chen G, Li XC, Wu GQ et al: The use of virtual reality for the functional simulation of hepatic tumors (case control study). *Int J Surg*, 2010; 8(1): 72–78
51. Javaux A, Bouget D, Gruijthuijsen C et al: A mixed-reality surgical trainer with comprehensive sensing for fetal laser minimally invasive surgery. *Int J Comput Assist Radiol Surg*, 2018; 13(12): 1949–57
52. Halic T, Kockara S, Bayrak C, Rowe R: Mixed reality simulation of rasping procedure in artificial cervical disc replacement (ACDR) surgery. *BMC Bioinformatics*, 2010; 11(Suppl. 6): S11